Restructuring the existing medium voltage distribution grids using DC systems

Shekhar, Aditya; Bauer, Pavol

Publication date
2022

Document Version
Final published version

Published in
Medium Voltage DC System Architectures

Important note
To cite this publication, please use the final published version (if applicable).
Please check the document version above.

Chapter 3

Restructuring the existing medium voltage distribution grids using DC systems

Aditya Shekhar[1] and Pavol Bauer[1]

3.1 Introduction

Typical distribution networks (DN) are predominantly AC and radial in nature, as shown in Figure 3.1. The voltage of a long distance high voltage (HV) network is stepped down to a medium voltage (MV) level at a substation located a few tens of kilometers outside an urban area. Power demand of the downstream network is delivered to an inner city substation using multiple parallel operating 3-phase AC links. Considering the critical function of this distribution link, adequate redundancy is employed to maintain the required power capacity during (n−1) contingencies, which refers to the operating condition with single component failure in the system.

3.1.1 Emerging challenges

Figure 3.1 highlights the emerging grid components such as electric vehicle chargers, traction systems and distributed generation resources like photovoltaics and wind farms. With mass deployment of such energy resources and high power loads, the existing grid infrastructure must be upgraded to meet the changing needs.

- Sustainable energy transition is leading to greater electrification. For example, it is anticipated that electrical energy demand will rise by at least 2–3 times by 2050 with increasing share of electric vehicles (EVs) and heat pumps [1]. Depending on the consumption patterns, this will translate to significant increase in peak power demand that can overload the critical AC power links in the system. In such systems, reinforcing the infrastructure with adequate redundancy for enhanced capacity during (n−1) contingencies becomes imperative.
- Dispersed and variable nature of renewable energy resources leads to power mismatch between generation and consumption even while the energy

[1]DC Systems, Energy Conversion & Storage group in the Department of Electrical Sustainable Energy, Delft University of Technology, Delft, The Netherlands
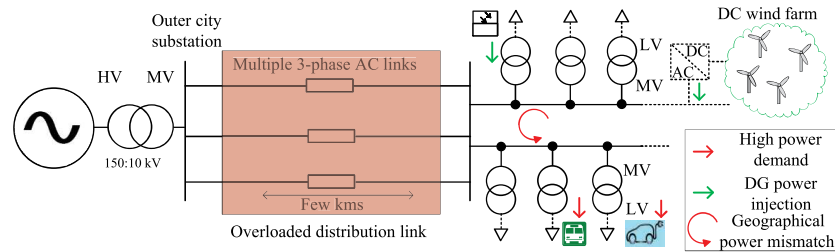
Figure 3.1   A typical medium voltage AC distribution network

dependence on the HV network is reduced. The radial structure of the MV distribution network further exacerbates the geographical mismatch associated with local pockets of excess power generation and consumption. In such operational scenarios, load balancing with efficient and controlled power redirection within the network is necessary.

- Direct integration and energy sharing between these components has led to the development of microgrid substructures capable of autonomous operation. The architecture of the point of common coupling between these microgrids and the main grid must handle operational challenges such as bidirectional power flows and protection aspects.

3.1.2   *AC distribution network expansion*

In response to growth in load, the Distribution Network Operators (DNOs) determine an optimal expansion plan to meet the future power demands. With network conductors as the main asset category, the decision on infrastructure reinforcement is a multi-objective consideration of trade-offs in investment cost, energy loss and reliability [2]. The three main constraints that must be satisfied during the problem formulation for expansion planning are (i) radial operation of the AC network, (ii) node voltage and branch current limits during normal operation, and (iii) adequate redundancy capacity during $(n-1)$ contingencies. Some operational flexibility to these constraints is introduced by considering the short duration overload capacity of the infrastructure and the possibility of reconfiguration using normally open tie-lines in the DN. According to [3], the hosting capacity of a radial DN downstream of a 11 kV, 10 MVA substation can be improved with optimal conductor sizing. The study defined a feeder reinforcement index corresponding to annual cost of energy losses relative to the investment cost and identified that the branch conductors closest to the substation needed to be upgraded with additional conductor cost compared to the base system. While re-conductoring and/or adding new multi-circuit AC branches is widely used by the DNOs for network capacity augmentation, almost 80% of the incurred costs are toward installation procedure (related to digging and routing) as compared to that of the actual cable material [4]. Further, the socio-economic difficulties can limit the practical viability of large-scale digging and installation of underground cable infrastructure, particularly in heritage

cities like Amsterdam in The Netherlands [5]. Different solutions have emerged to address the need for deferring the DN capacity investments:

- **Energy Storage System (ESS)** can be a non-wire alternative to achieve peak demand shaving to prevent overloads in the network upstream of the installation node. For example, Deboever et al. [6] investigated the increase in the required energy and power capacity of the ESS as a function of current clipping objective including the impact of load growth for an actual 27.6 kV, 15 MVA feeder. The study suggested that a 15% peak shaving of current overload can be achieved with a 16.6 MWh, 2.5 MW ESS. A cost–benefit analysis for different 20 kV DN suggested that the target ESS cost of 60–80 €/kWh can be considered as a competing solution to traditional network reinforcement [7]. The paper anticipated a decline in future storage costs, use of second life batteries and increased penetration of EVs as possible scenarios where ESS based capacity reinforcement of secondary substations can be considered as an attractive solution.
- **Distributed Energy Resources (DERs):** While the variable nature of generation with DERs can cause grid congestion, their optimal location, sizing and operation in coordination with DN planning can be beneficial in addressing load growth. For example, an integrated approach of installing DERs along with upgrading tie-lines, conductor and transformer can offer 10% savings over a 20 year investment horizon [8]. The assumption is that the installed DER is able to supply power during peak load requirements in the system. A dynamic improvement of inter-area power transfer capability is suggested in [9] for under-utilized grid infrastructure under low wind conditions. However, some regulations prohibiting the DNOs from owning generation plants may lead to potential inefficiencies in supply infrastructure because the role of DERs in deferring investments of network expansion maybe overlooked as a consequence [10]. A distributed ownership of resources can, therefore, necessitate some degree of coordination between different stakeholders. The concept of prosumer based on clustered micro-generators could be used, especially with autonomous transaction with bitcoins/smart-meters.
- **Smart Loads:** Controllable power electronics assisted loads can offer some flexibility to address the supply challenges. Smart charging of electric vehicles and intelligent heating systems can shape the consumption patterns to relieve and/or support the DN during peak demand hours. It is observed that while the EV hosting capacity of a test DN can be maximized within the defined chargeable region with electricity price based demand response (DR), the capacity violations cannot be completely prevented [11].

A combination of aforementioned solutions along with use of Information and Communication Technologies (ICT) has led to the development of Demand Side Management (DSM) concept for smart grids [12]. Recognizing the limitation of market based DR in completely alleviating congestion, it is mixed with binding physical DR requests of load shedding for grid relief.

3.1.3 DC technology based solutions

The role of DC technologies in enabling smart grids is three-fold: (i) higher infrastructure efficiency and power density as compared to AC; (ii) potential for greater inter-connectivity as compared to conventional radially-constrained AC DN in power redirecton and improving availability; (iii) efficient integration because most emerging grid resources like ESS, DERs and EVs have intermediary DC conversion stage. This understanding has led to research initiatives in the control, protection and architectural design of DC distribution and microgrid systems [13]. However, the possibility of large-scale deployment of multiterminal DC grids at medium voltage level by DNOs is impeded by the cost of ownership and operational maturity with the existing AC infrastructure [14]. Therefore, the subsequent sections introduce working solutions for restructuring the existing AC grids with an objective of increasing the DC based distribution technologies in these systems.

This chapter emphasizes the role of DC technologies in achieving grid transition as an important step to realize sustainable energy transition. The discussed principles are applicable for MV levels of 10–66 kV, short link lengths space in between a few tens of kilometers and distribution system power capacities in the range of a few MWs. The proposed concepts have potential practical applications, for example in Siemens approach with 'MVDC Plus' [15].

3.2 Refurbishing AC infrastructure for DC operation

This section discusses the conventional solutions for AC DN planning to address the challenge of load growth. The potential power capacity gains by converting the AC infrastructure for DC operation is presented and the research opportunities on this topic are highlighted.

3.2.1 Capacity enhancement with DC operation

The existing AC conductor infrastructure can be refurbished to operate under DC conditions by AC/DC converters on either side of the link as shown in Figure 3.2.

The refurbishment strategy is proposed for operating branches as well as normally open tie-lines which can potentially reduce future overloads in the network [16]. Capacity enhancement can be achieved without installation of additional link conductors because DC operation has inherently higher power density as compared to AC as indicated in Figure 3.3.
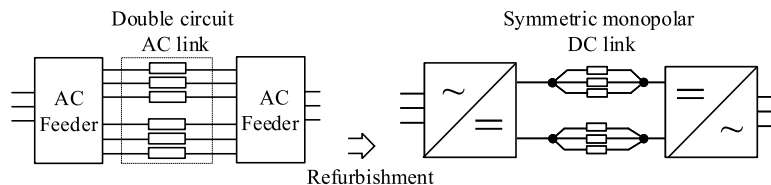

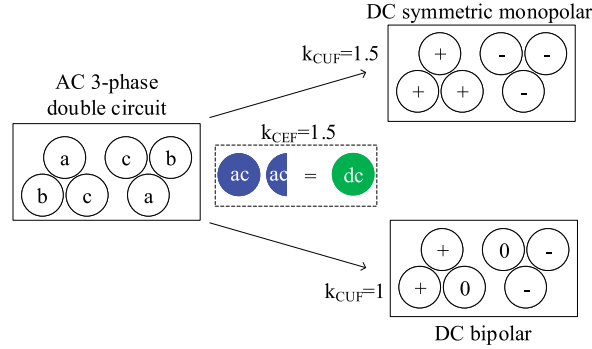*Figure 3.2   Refurbishing AC links for DC operation*

Figure 3.3   Power capacity enhancement by converting AC circuit for DC operation

The capacity enhancement factor k_{CEF} represents the amount of conductor area required to transfer AC power equivalent to that under DC operation. In the shown case, the value indicates that 1.5 times more AC conductor area is required to transfer the equivalent DC power. In general, the approximate k_{CEF} can be estimated from (3.1):

$$k_{CEF} = k_{vr} \underbrace{\left(\frac{v_{dc}}{v_{ac}}\right)}_{k_v} \underbrace{\left(\frac{i_{dc}}{i_{ac}}\right)}_{k_i} \underbrace{\left(\frac{1}{\cos\theta}\right)}_{k_{pf}} \tag{3.1}$$

Herein, the voltage enhancement factor k_v is defined based on the link insulation performance as a ratio of the pole to ground DC voltage v_{dc} and phase to ground AC voltage v_{ac}. While a conservative estimate of $k_v = \sqrt{2}$ can ensure similar or better insulation performance under DC as compared to AC [5,17], the possibility of selecting higher values of k_v to achieve significant capacity enhancements have been reported in the literature [18,19]. The factor k_i accounts for the current rating enhancement with DC operation. For short link lengths typical of medium voltage levels, k_i is in the range of 1.01–1.03 based on the skin affect associated with conductors of different cross-sectional area, while for systems with longer link lengths, the influence of capacitive currents can result in a higher value. Further, k_i can be higher if the AC to DC refurbishment impacts the derating associated with the thermal proximity of the link conductors. The factor k_{pf} incorporates the influence of reactive power support provided by the Voltage Source Converter (VSC) at the receiving end of the refurbished DC link. Assuming a minimum power factor $\cos\theta = 0.9$, k_{pf} is in the range of 1–1.1. Finally, the factor k_{vr} is associated with the voltage regulation and link length dependent inductive voltage drop and is in the range of 1.03–1.05. A discussion on the influence of varying system parameters and operating conditions on these factors is offered in [5], which forms the basis for the assumption that $k_{CEF} = 1.5$ is a reasonable conservative estimate for DC capacity enhancement.

The actual system level capacity enhancement is described by the conductor utilization factor k_{CUF} depending on the topology of the original AC link, the

refurbished DC link and the selected substation converter rating. It is related to k_{CEF} by (3.2):

$$k_{CUF} = k_{cr} \left(\frac{N_{dc}}{N_{ac}} \right) k_{CEF} \tag{3.2}$$

N_{ac} and N_{dc} are the number of active conductors involved in high power transfer for original AC and refurbished DC link respectively. For example, if a three-phase AC link is converted to a 2-pole DC link, then $N_{ac} = 3$ and $N_{dc} = 2$ resulting in a reduced k_{CUF} relative to the k_{CEF}, leading to lower achievable capacity gains with the refurbishment strategy.

The converter rating factor k_{cr} is defined as the ratio of rated converter active power to the maximum achievable active power capacity of the DC link conductors. The value of k_{cr} influences the installation cost of the substation converters and can be selected based on the required capacity enhancement in the system. With maximum possible value of $k_{cr} = 1$ and a conservative $k_{CEF} = 1.5$, it can be seen from Figure 3.3 that while no capacity enhancement is achieved when a three-phase double circuit AC link is refurbished to a bipolar DC link with two neutral conductors, 1.5 times higher capacity is achieved when it is refurbished to a symmetric monopolar DC system. A review of capacity enhancement claims in the literature are listed in Table 3.1.

While all listed studies reported a k_{CEF} above 1.5, the contributing factors and assumptions based on the system parameters are different. For example, the field implementation in [4] selected the most conservative DC voltage enhancement k_v and still achieved a higher k_{CEF} because the operating line current was increased from 66 A AC to 150–300 A dc. On the other hand, the case-study in [18] suggests that the achieved DC capacity gains were because voltage drop associated with long link length limited the transmission capacity of the original AC system below the thermal limit. Both [4,18] suggest that a higher DC voltage enhancement can be selected with consideration to the consequences on insulation performance. Based on empirical evidence provided in [20], $k_v = \sqrt{2}$ can offer capacity gains that are independent of link length as suggested in [5,17].

A higher AC to DC voltage enhancement potential ($k_v > \sqrt{2}$) is an important consideration for medium voltage DNs because short links dominate such systems

Table 3.1   Capacity enhancement claims with refurbished DC link operation

References	k_{CEF}	k_v	$v_{ll,rms}$	Capacity	Length	Type
			(kV)	(MVA)	(km)	
[4]	1.5–6.0	0.5–1	35	3	40	Cable
[5]	$\geq$1.5	$\sqrt{2}$	11	10–30	10–20	Cable
[17]	1.59	$\sqrt{2}$	10	10–20	–	Cable
[18]	1.63	1.18	66	70	18	Overhead
[19]	3.5	$2\sqrt{3}$	145–420	100–2,500	>100	Overhead

and therefore, the capacity gains associated with voltage regulation and capacitive current are limited. Ref. [19] is one of the early works supporting AC to DC refurbishment strategy for extremely high voltage overhead networks. While the study considers a much higher k_v, the suggested value is corresponding to the modification of supporting tower and insulation structures of the overhead transmission system. A similar principle is being explored for medium voltage overhead distribution lines in [15]. However, the appropriate choice of k_v must correlate similar insulation performance under AC and DC voltages, particularly for underground cable systems as discussed in Section 3.2.4.

3.2.2 Operational considerations

The defined factor k_{CUF} represents the capacity enhancement during normal system operation. During (n−1) contingencies, introducing reconfigurability between the refurbished AC–DC link systems can be seen as a method to maximize the utilization of the remaining healthy infrastructure to reduce the need for redundancy in the system [21]. This is advantageous because the added cost of redundancy has limited use during normal conditions where the system spends the majority of its operational lifetime. Figure 3.4(a) shows the reconfigurable AC–DC link architecture where the feeder switches can regulate the physical AC and DC power flow path between the Sending end Sub-Station (SSS) and the Receiving end Sub-Station (RSS) via the existing link conductors. The AC–DC reconfiguration based service restoration and design of selective protection scheme for fault isolation is an important research topic and some discussion on the possible opportunities and challenges will be discussed in the subsequent sections.

Figure 3.4(b) depicts a parallel AC–DC link system between SSS and RSS. Such systems inevitably emerge with partial AC to DC refurbishment wherein only some of the multiple AC links (refer Figure 3.1) are converted for DC operation [22]. Further, the reconfigurability between AC and DC operation can offer flexibility in choosing the system architecture for a given active and reactive power (P, Q) demand at the RSS. The optimal active power sharing (P_{ac}, P_{dc}) between the AC and DC link systems is a function of dynamically varying operating efficiency. The control objective of the RSS side VSC is to steer the active power in the system at the maximum efficiency while supporting the reactive power needs in the system for a given AC–DC configuration.
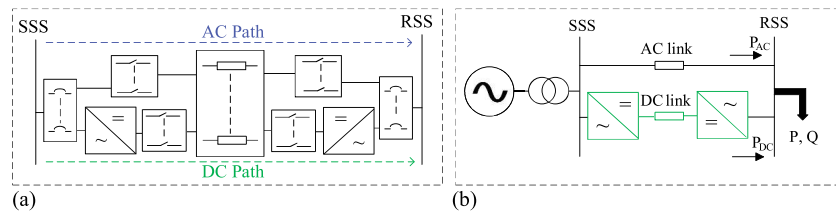

(a)   (b)

Figure 3.4   Operational considerations with (a) reconfigurability between AC and DC links and (b) parallel AC–DC operation

3.2.3   Converter station design considerations

The substation converters must be rated according to the maximum demand that they are expected to deliver during normal operation as well as (n−1) contingencies. k_{cr} can be reduced while maintaining the same system capacity based on the operational mode selected such as parallel AC–DC operation and the reconfiguration strategy employed when a fault occurs [23]. For example, it is discussed that the required converter station capacity can be downsized by more than 50% to maintain the same system capacity during (n−1) contingencies if a re-configurable architecture shown in Figure 3.4 is used. While the advantage of this derating opportunity is the significant reduction in installation costs, it can reduce the system efficiency under normal operating conditions because DC power transfer can be more efficient under specific situations. This trade-off must be investigated by the DNOs for proper sizing of the refurbished parallel AC–DC link converter stations depending on the annual load profile at the RSS.

Figure 3.5 shows two different converter station architectures that can used for DC link system.

In Figure 3.5(a), a common DC bus supplies power with each DC pole connected to $N_{dc}/2$ conductors. This architecture is similar to the one shown for refurbished DC system in Figure 2.2. Alternatively, $N_{dc}/2$ independently operating DC links can be formed as shown in Figure 2.5(b). There are three important research considerations that influence the choice between these architectures (i) The number of converters N_{conv} and rating of each can be optimized in case of common DC bus based on the functional and modularity requirements of the system while for independent DC links, at least $N_{dc}/2$ converters must be present, (ii) if AC circuit breakers are used to isolate the DC conductor to ground faults, modularity offered by independent DC link operation can limit the load shedding during fault isolation process, and (iii) if the VSC station architecture is employed within the reconfigurable AC–DC system shown in Figure 3.4(a), common DC bus approach can simplify the AC and DC feeder switching scheme. Therefore, the selected architecture can influence converter cost, capacity of the system during (n−1) contingencies, protection, and the reconfigurable switching scheme. Some discussion on VSC configuration on capacity enhancement with DC refurbishment scheme is presented in [24].

Finally, the selection of topology and components of the operating converter relevant to this medium voltage and high power application is important. With current
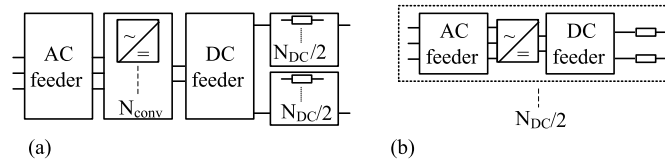

| (a) | (b) |

Figure 3.5   Converter station architecture (a) common DC bus and (b)
          independent dc links

power electronic technologies, use of VSCs has implicitly been assumed in this discussion and operation with more than two-levels can have advantages. Neutral point clamped (NPC-VSC) have acceptable performance up to three to five levels. Further, use of multilevel H-bridge converters have also shown promise [25,26]. The performance parameters of multilevel converters with optimum number of levels as a function of grid voltage is offered in [27]. An operating efficiency above 99% can be expected for Insulated Gate Bipolar Transistor (IGBT) switch based half-bridge Modular Multilevel Converter (MMC) as per the design considerations for optimum number of levels presented in [28,29]. The potential application of new semiconductor technologies can be an interesting research topic.

3.2.4   Link conductor considerations

The insulation performance under AC and DC medium voltages is important to determine the acceptable voltage enhancement factor k_v. The corresponding capacity enhancement estimates may be different for insulation types, overhead and cable infrastructure and joints and accessories of the link system. In general, it is expected that a much higher DC operating voltage can be imposed as compared to AC considering partial discharges as an insulation performance indicator [30]. While preliminary empirical studies comparing insulation performance under AC and DC voltages support this expectation [20], it is difficult to estimate the accurate DC voltage enhancement factor ensuring safe operation without detrimental effect to insulation lifetime over several years. Therefore, with field implementation of the suggested AC to DC refurbishment strategy, a gradual increase in k_v is recommended [4].

Further, it is known that space charge accumulation can result in local electric field enhancement and even inversion within the insulation under DC voltages. Based on qualitative understanding, the detrimental effect on insulation lifetime in case of frequent and sudden polarity reversal may encourage minimization of DC to AC reconfiguration during (n−1) contingencies. However, many aspects need further investigation, such as: (i) magnitude of accumulated space charges at medium voltage levels (translated to imposed electric fields on the insulation) [31]. These are possibly low at the considered voltage levels and therefore, less significant. (ii) Time and temperature dependence of space charges when DC voltage is imposed or removed [32]; (iii) insulation performance under the expected space charge accumulation at different locations in cable insulation system over its operational lifetime (iv) understanding of impact on insulation with DC to AC reconfiguration based on (a) reconfiguration frequency and (b) time-lag after each such reconfiguration. Such performance indicators must be investigated with different insulation systems (example: XLPE, EPR) [33]. Keeping these considerations in mind, incremental gathering of on-field operational know-how as recommended in [4] is particularly important.

3.3   Parallel AC–DC link operation

Consider the original AC system operating with three-phase AC links as shown in Figure 3.6(a). It can be inferred that with a base power corresponding to a single
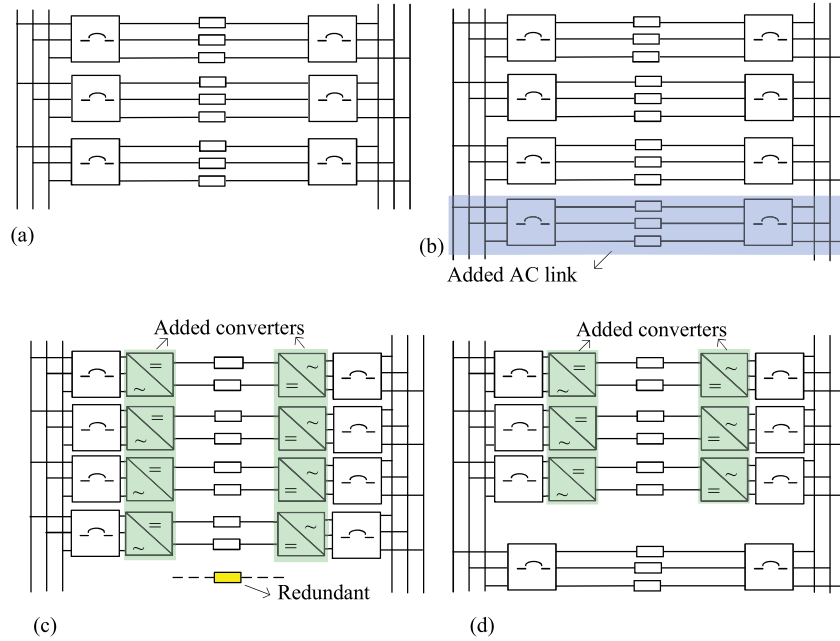
Figure 3.6   Different capacity enhancement strategies: (a) original system
(N_{ac} = 9, N_{dc} = 0); (b) configuration C0 (N_{ac} = 12, N_{dc} = 0);
(c) configuration C1 (N_{ac} = 0, N_{dc} = 8); (d) configuration C2
(N_{ac} = 3, N_{dc} = 6)

3-phase AC link, this system has a capacity of 3 p.u. during normal operation and 2 p.u during (n−1) contingencies because two healthy AC links remain after fault isolation when a single component failure occurs. Conventionally, an AC link is added to increase the capacity of this system to 3 p.u. during (n−1) contingency, shown as configuration C0 in Figure 3.6(b).

Figure 3.6(c) and (d) shows two different DC refurbishment strategies with N_{ac} = 0, N_{dc} = 8 (configuration C1) and N_{ac} = 3, N_{dc} = 6 (configuration C2) respectively. For k_{CEF} = 1.5, both systems are capable of delivering a power demand of 3 p.u. during (n−1) contingencies. While the post-fault reconfigurability between AC and DC link conductors is not shown here, both refurbishment schemes are incorporated within the reconfigurable architecture illustrated in Figure 3.4(a). Assuming that the configurations shown in Figure 3.6(b)–(d) can be imposed with a maximum system power demand of 3 p.u. during normal conditions and operate at maximum efficiency, the total converter rating must be 3 p.u. for C1 and 2.25 p.u. for C2 for substation at each end. Therefore, the converter costs are about 25% lower for parallel AC–DC (C2) as compared to complete DC (C1) refurbishment for maintaining the same system capacity during (n−1) contingencies.

Table 3.2   System parameters and assumptions

Parameter	Value
AC grid voltage (line to line)	10 kV
DC link voltage (pole to pole)	16.33 kV
Type, cross-sectional area and current rating of link conductor	Al, 400 mm 2,450 A
Base power	7.8 MVA
Required system capacity during (n−1) contingencies	3 p.u at power factor pf=0.9
Converter efficiency	99.34%
Cost[†] of installing a 3-phase AC link ($f_{c,cond}$)	100 per m
Cost[†] of converter station ($f_{c,conv}$)	50 per kVA
Cost of space requirements ($f_{c,s}$)	50,000 per station
Energy cost	0.1 per kWh

[†]A sensitivity analysis to the assumed cost parameters is offered in [22].

Table 3.3   Viability boundaries for different capacity enhancement strategies

	Zone 1	**Zone 2**	**Zone 3**	**Zone 4**	**Zone 5**
Most efficient	C0	C2	C2	C1	C1
Economically viable	C0	C0	C2	C2	C1

Consider the operating system parameters and assumptions listed in Table 3.2 with the objective to select the optimal grid reinforcement strategy (C0, C1, or C2) to enhance the capacity of the system shown in Figure 3.6(a) from 2 p.u. to 3 p.u.

The DC link pole-to-pole voltage (v_d) can be calculated from the r.m.s. line to line AC line voltage ($v_{ll,rms}$) from (3.3):

$$v_d = \frac{2k_v v_{ll,rms}}{\sqrt{3}} \tag{3.3}$$

The DC link of the parallel AC–DC configuration can be used to steer the active power in the system depending on the RSS demand (P_{RSS}). The approximate share (y_{approx}) of DC active power P_{dc} to operate the system at optimal efficiency is given by (3.4):

$$y_{approx} = \frac{P_{dc}}{P_{RSS}} = \frac{k_v N_{dc}}{N_{ac} + k_v N_{dc}} \tag{3.4}$$

For example, $y_{approx} \approx 0.74$ when $k_v = \sqrt{2}$ is selected for configuration C2 (refer Figure 3.6d). Here, y_{approx} is calculated by taking into account solely the power carrying capacity of the AC and DC link conductors and assuming that the substation converters are rated to deliver this power. The optimal efficiency point of DC power share y_{opt} varies as a function of the operating parameters such as RSS active and reactive power demand, converter efficiency, link length and conductor area. The dynamic deviation of y_{opt} from y_{approx}, which is further constrained by the substation converter size (k_{cr}) is explored in [34].
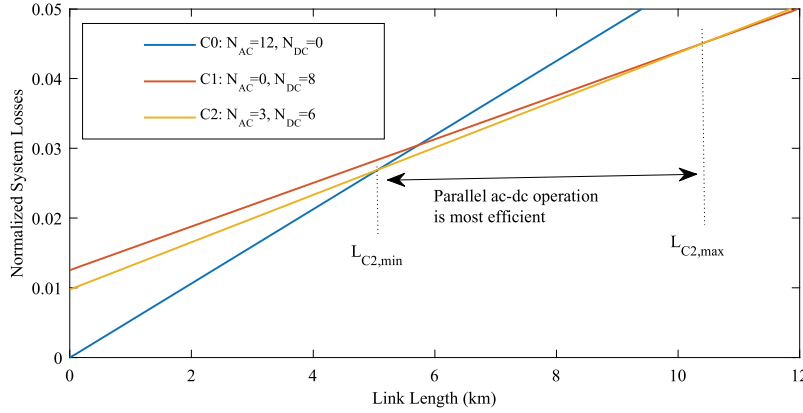
*Figure 3.7   Normalized system losses for different grid reinforcement strategies
with varying link length for RSS demand of 23.4 MVA at pf=0.9*

Based on the AC and DC link conductor currents i_{ac} and i_{dc} respectively, the system losses ($P_{loss,sys}$) for the given link length l, conductor resistance per unit length (r_{ac}, r_{dc}) and the RSS power demand is given by (3.5):

$$P_{loss,sys} = N_{ac}i_{ac}^2 lr_{ac} + N_{dc}i_{dc}^2 lr_{dc} + P_{loss,conv} \tag{3.5}$$

Here, $P_{loss,conv}$ is the sum of the total SSS and RSS converter loss in delivering the DC link active power while supporting the reactive power demand. It can be estimated that with RSS demand of 3 p.u. at pf=0.9, the normalised $P_{loss,conv}$ is 0.0125 p.u. for configuration C1 and 0.0097 p.u. for configuration C2 for the operating parameters mentioned in Table 2.2. Correspondingly, using (2.5), the variation of system losses for capacity enhancement strategy C0 (added AC link), C1 (complete DC refurbishment) and C2 (parallel AC–DC refurbishment) as a function of l is shown in Figure 3.7.

The observed slope is different for the three grid reinforcement strategies because AC link conductor losses per unit length are higher than DC for the given operating conditions. As a consequence, C0 has the highest loss variation with link length, followed by C2 and C1, respectively. For lower link lengths the converter losses dominate in DC operation, and these are lower for C2 as compared to C1 because the share of power transferred by the DC link is lower for the former. It can be observed that the indicated crossover points $L_{C2, min}$ and $L_{C2, max}$ describe the length range between which parallel AC–DC operation is the most efficient. For $l < L_{C2, min}$, AC reinforcement strategy C0 is most efficient, while complete DC refurbishment C1 is most efficient for $l < L_{C2, min}$. The variation in $L_{C2, min}$ and $L_{C2, max}$ depends on the AC grid voltage, DC link voltage, power demand at RSS, share of AC and DC power transfer, converter efficiency, number of conductors and their cross-sectional area. The associated mathematical relationship and sensitivity analysis is described in [22].

The economic choice between the reinforcement strategies depends on the 10 year payback associated with the operating losses for the given load demand and
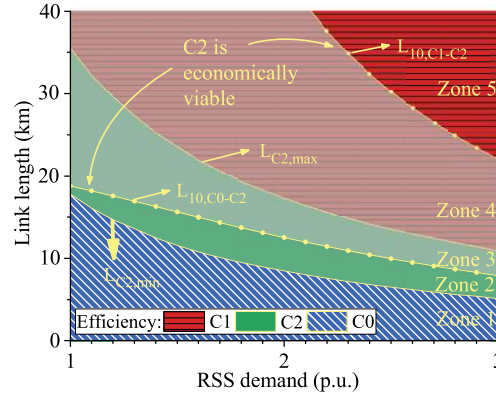
*Figure 3.8   Viability boundaries for a 10 year payback period with varying link
lengths and RSS demand at pf=0.9 (copyright: [22])*

incurred investment costs. For the given configuration, the total cost of installation
($f_{c,ins}$) is given by (3.6):

$$f_{c,ins} = f_{c,cond}l + f_{c,conv}S_{conv} + f_{c,s} \tag{3.6}$$

The installation costs increase with link length for AC reinforcement strategy
C0 (1 M€ for $l = 10$ km and double this value for $l = 20$ km). The installation cost
for DC refurbishment strategies are independent of link length and depend on the
chosen converter rating. Since the maximum converter rating for C2 is approxi-
mately 75% of C1, its $f_{c,ins}$ is 1.85 M€ as against 2.44 M€ for the latter. These
values are based on the cost assumptions described in Table 3.2. The economic and
efficiency boundaries for selecting the appropriate capacity enhancement strategy
with varying average RSS demand and link length is shown in Figure 3.8.

The four plot-lines, $L_{C2, min}$, $L_{10,C0-C2}$, $L_{10,C1-C2}$ and $L_{C2, max}$, divide the graph
area into five zones. Herein, $L_{10,C0-C2}$ describes the link length above which the
return on higher investment with C2 has a 10 year simple payback as compared to
C0. Similarly, $L_{10,C1-C2}$ describes the link length above which the return on higher
investment with C1 has a 10 year simple payback as compared to C2. The observed
efficiency and economic viability boundaries for zones 1–5 are listed in Table 3.3. In
zone 1, installing an additional AC link is the most efficient and economic solution.
Similarly, in zones 3 and 5, DC refurbishment with C2 and C1 are the most viable
capacity strategy respectively. The transitional zones 2 and 4 describe the region
where an increase in DC capacity can be more efficient but not economically viable.

The conclusion is that the break-even distance between AC and DC power transfer
is a smooth transition wherein parallel AC–DC operation can be the most economic
choice for a band of link lengths described by Zone 3 ∪ Zone 4. The width and
boundaries of this viability band can shift with different system parameters and cost
assumptions than those listed in Table 3.2. Particularly at medium voltage levels of
10–66 kV, short link lengths up to a few tens of kilometers and capacities in the range

of few MWs, power transfer with parallel AC–DC operation is preferred as compared to solely AC or DC transmission within this multi-dimensional viability band.

3.4   Reconfigurable AC–DC link architecture

Consider the refurbishment of a double circuit AC link to DC operation shown in Figure 3.2, wherein the entire system must be shut down in case a converter fault occurs. By providing modularity as suggested in Figure 3.5, some system capacity can be preserved during faults. Protection design aims to isolate the faulty component and restore the operation of the remaining healthy infrastructure as soon as possible to minimize the magnitude and duration of load shedding. Adequate redundant infrastructure is installed to ensure that the required capacity can be maintained during $(n-1)$ contingencies. While increased modularity can reduce the need for redundancy, this method has both practical and cost limitations. For example, increasing the number of converters N_{conv} in Figure 3.5(a) significantly increase the number of power electronic components, which is detrimental to reliability, space requirement and unit system cost. Similarly, modularity in number of point-to-point DC links suggested in Figure 3.5(b) is limited to $N_{dc}/2$ by the number of link conductors and the loss in capacity is equivalent to a single DC link, which translates to increased incurred cost of redundancy.

Another way of minimizing the cost of necessary redundancy is to introduce reconfigurability in the system architecture. This offers post-fault flexibility to maximize the functional utilization of the remaining healthy infrastructure. For example, if the same converter fault occurs in a reconfigurable system, the healthy DC link conductors can be re-utilized in AC operation to enhance capacity. The concept is depicted in Figure 3.9, where the six link conductors x_1-x_6 can operate either in AC or DC condition by choosing the state of feeder switches connecting the AC and DC bus at the substation.
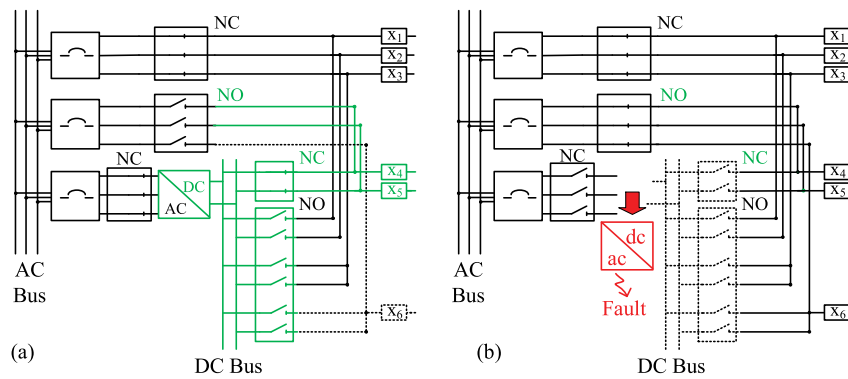

Figure 3.9   Re-configurable ac–dc architecture (a) normal operation and (b) AC bypass during converter faults

Figure 3.9(a) depicts the normal operation with x_1-x_3 forming a three-phase AC link, x_4-x_5 operating as DC link and x_6 is a redundant conductor. This is a possible refurbishment strategy with one of the double circuit AC link (refer Figure 3.2 for original AC system) converted to DC operation. It can be inferred that without reconfigurability, the k_{CUF} of this system during normal operation is equal to 1. Further, a single component failure anywhere in the system results in the loss of one line and therefore, no capacity enhancement over the original AC system could be achieved even with DC refurbishment. However, Figure 3.9(b) shows that when a converter fault occurs, conductors x_4-x_6 can be re-connected to the AC bus after isolating the DC bus to form a second three-phase AC link. Therefore, the capacity of this system is increased to twice due to AC–DC reconfigurability in operation.

Similarly, when a link conductor to ground fault occurs in the system initially operating in the state shown in Figure 3.9(a), reconfigurations can improve the maintainable capacity. Figure 3.10(a) shows that when a short circuit occurs in the AC conductor x_3, it is isolated and the feeder switches are reconfigured such that $x_4 - x_6$ form the new AC link while $x_1 - x_2$ form the DC link in the post-fault scenario. Figure 3.10(b) shows the scenario where x_6 replaces the faulty DC link conductor x_5. The capacity is improved in both considered (n−1) contingencies because the AC and DC links can function at their design rating even with a single component failure.

Reconfiguration strategies with different types of fault scenarios, the related converter downsizing potential and trade-off with operating efficiency of the system is discussed in [35]. The study shows that with use of reconfigurability, the substation converters can be downsized by as much as 75% to achieve the same required capacity during (n−1) contingencies. However, this reduction in converter size decreases the system efficiency during healthy operating conditions because the DC link is unable to operate at its optimal power share. Considering that the system is expected to operate in normal conditions for most of its lifetime, a 10-year simple
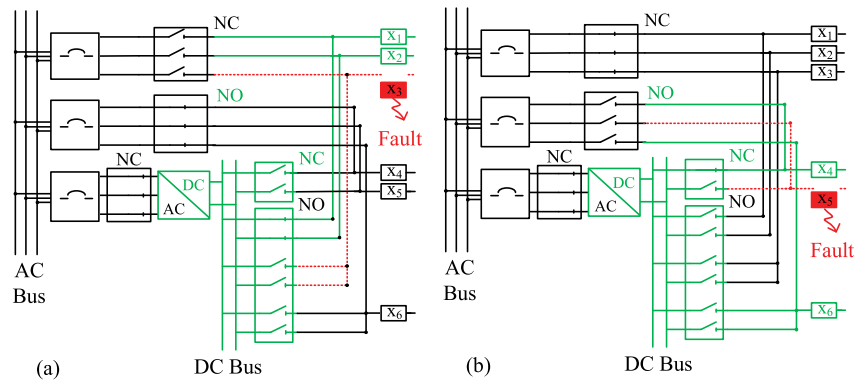

Figure 3.10   Reconfigurability during (a) AC conductor to ground fault and (b) DC conductor to ground fault

payback calculation suggests that the potential for converter de-rating increases with increasing grid voltage and decreasing link length of a refurbished parallel AC–DC system operating within a reconfigurable architecture proposed in Figure 3.4(a).

Consider a system originally operating with $N_{\text{ac,ori}}$ AC conductors. Using base power equivalent to a single three-phase AC link ($P_{\text{base}} = 3v_{\text{ac}}i_{\text{ac}}$), the per unit system capacity during normal operation is $N_{\text{ac,ori}}/3$ and that during (n−1) contingency is $(N_{\text{ac,ori}} - 3)/3$. For example, with $N_{\text{ac,ori}} = 6$, the system can deliver a maximum power of 2 p.u. during normal operation and 1 p.u. when a single AC link fails. Since the number of AC conductors is a multiple of three and number of DC conductors is even, the original system can be refurbished to DC in $N_{\text{ac,ori}}/3$ possible configurations while ensuring that the number of redundant conductors (N_{red}) is minimum. The resultant number of operating AC and DC conductors is given by (3.7) and (3.8), respectively:

$$N_{\text{ac}} = (n-1) * \left(\frac{N_{\text{ac,ori}}}{3} \right) \tag{3.7}$$

$$N_{\text{dc}} = \begin{cases} N_{\text{ac,ori}} - N_{\text{ac}}, & \text{if } N_{\text{ac,ori}} - N_{\text{ac}} \text{ is even} \\ N_{\text{ac,ori}} - N_{\text{ac}} - 1, & \text{otherwise} \end{cases} \tag{3.8}$$

Here, n can take integer values between 1 to $N_{\text{ac,ori}}/3$ and the possible refurbished AC–DC configurations for different $N_{\text{ac,ori}}$ are listed in Table 3.4. k_{CUF} and $k_{\text{CUF,n−1}}$ indicate the capacity enhancement corresponding to the fixed refurbished DC configuration compared to the original AC system during normal and fault conditions respectively. For a $k_{\text{CEF}} = 1.5$, the k_{CUF} and $k_{\text{CUF,n−1}}$ can be derived from (3.2), given by (3.9) and (3.10) respectively:

$$k_{\text{CUF}} = \frac{\left(\frac{N_{\text{ac}}}{3} \right) + \left(\frac{N_{\text{dc}}}{2} \right) k_{\text{cr}}}{\left(\frac{N_{\text{ac,ori}}}{3} \right)} \tag{3.9}$$

$$k_{\text{CUF,n−1}} = minimum \left(\frac{\left(\frac{N_{\text{ac,n−1}}}{3} \right) + \left(\frac{N_{\text{dc,n−1}}}{2} \right) k_{\text{cr,n−1}}}{\left(\frac{N_{\text{ac,ori,n−1}}}{3} \right)} \right) \tag{3.10}$$

Table 3.4 AC–DC reconfigurations, converter size and capacity enhancement with refurbished DC operation

$N_{\text{ac,ori}}$	N_{ac}	N_{dc}	N_{red}	P_{conv}	k_{cr}	k_{CUF}	$k_{\text{CUF,n−1}}$	$k_{\text{CUF,n−1,r}}$
6	0	6	0	3 p.u.	1	1.5	2	2
				2 p.u.	0.67	1	1.33	2
	3	2	1	1 p.u.	1	1	1	2
9	0	8	1	4 p.u.	1	1.33	1.5	2
				3 p.u.	0.75	1	1.125	1.5
	3	6	0	3 p.u.	1	1.33	1.5	1.5
				2 p.u.	0.67	1	1.167	1.5
	6	2	1	1 p.u.	1	1	1	1.5

Here, the converter rating factor $k_{cr} \geq 1$ is determined by the installed substation converter power rating (P_{conv}) as the ratio of the total DC link conductor power for the given operating configuration. $N_{ac,n-1}$, $N_{dc,n-1}$ and $k_{cr,n-1}$ depend on the state of remaining conductors and converters after AC conductor, DC conductor or a converter fault occurs respectively. $k_{CUF,n-1}$, therefore, describes the capacity enhancement factor of a given configuration during (n−1) contingencies. $k_{CUF,n-1,r}$ is the achievable capacity enhancement factor if post-contingency reconfigurability between AC and DC operation is employed.

It can be observed from Table 3.4 that decreasing P_{conv} results in a decrease in k_{CUF} and $k_{CUF,n-1}$ for the given configuration. However, if reconfigurability is introduced, the converter can be significantly downsized even while maintaining the same system capacity enhancement ($k_{CUF,n-1,r}$). For example, a system with $N_{ac,ori} = 9$ has 2 p.u. capacity during (n−1) contingencies. Three DC refurbishment strategies are possible and as installed converter rating is varied between 1 and 4 p.u., a post-contingency capacity of 3 p.u. ($k_{cr,n-1,r} = 1.5$) can be maintained using re-configurations, leading to a potential of about 75% cost reduction. However as a result, the trade-off in lower operating efficiency during normal conditions (as described in Figure 3.8) is important to consider over the system lifetime.

3.5 Hybrid AC–DC distribution systems

3.5.1 DC interlinks in radial networks

The concept of DC based active power routing in the DN is shown in Figure 3.11. Here, a Back-To-Back Modular Multilevel Converter (BTB-MMC) based DC interlink can control the bidirectional power flow between nodes 6 and 8 of the network. Further, the power electronic converters at each node can offer ancillary services to the connected grid, such as fault ride through, reactive power and voltage support. In practice, this restructuring can be realized either by refurbishing existing tie-lines or by installing a new DC link interconnection between selected nodes in the system, depending on the economic viability in relation to the functionalities offered.

Conventionally, Normally Open (NO) tie lines in AC distribution systems are used for network reconfiguration to achieve load balancing, loss reduction and service restoration [37–39]. While these studies investigate the optimal branch switching configuration to realize the mentioned objectives for given power flows in the DN, a radial constraint is imposed on the selected operating topology. Weakly meshing such systems with limited number of loops can improve functionality and toward this concept, the DC interlink can provide an efficient and controllable capacity enhancement solution. For example, it is shown that the DN losses of a 33-bus weakly meshed system reduce with increasing DC power transfer as compared to the radial network with similar load powers at the nodes [36]. The power flow between bridged feeders in a radial network was regulated using controllable back-to-back VSC based DC links to show that the loadability improved by about 150% as compared to the base case [40]. The paper showed that assuming
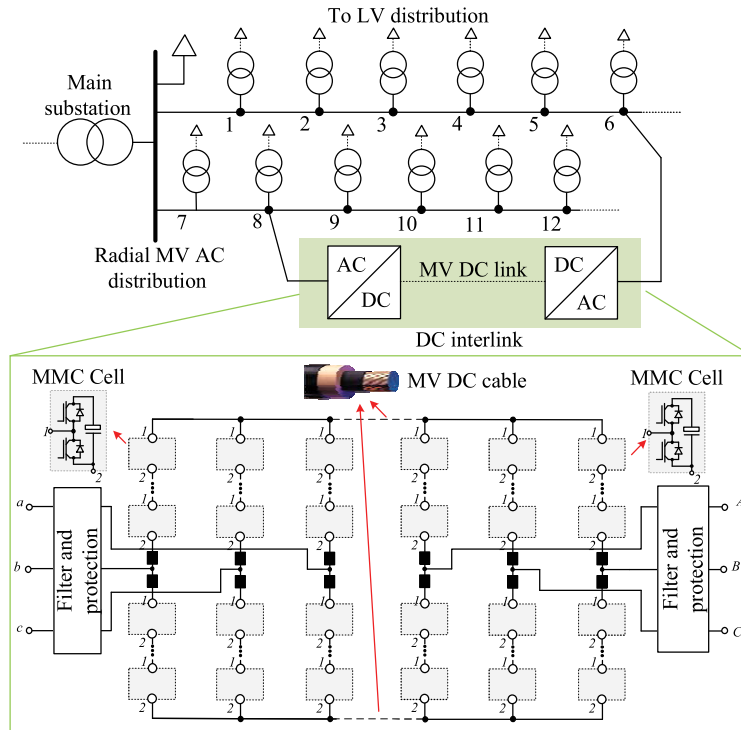
Figure 3.11   Power electronics assisted DC interlink based power redirection in radial AC distribution networks (adapted from [36])

a installed 6 MVA DC link technology cost of 250 €/kVA, a payback of 1.4 years is possible because of extra income due to 21% increase in peak PV power with improved DG penetration. Extending the concept, it was shown that storage integrated DC interlink can improve voltage at remote terminals, reduce feeder transformer loading by 50% and reduce system losses by 2–4% with increasing photovoltaic (PV) power generation [41].

The emerging hybrid AC–DC DN is fundamentally a composite version of a parallel AC–DC system shown in Figure 3.4 (b) and therefore, the underlying principles discussed in Section 3.3 are applicable. In this context, the sizing and placement of the DC interlink in a given AC DN is a multi-objective optimization considering the efficiency and capacity gains with DC power redirection in addition to the ancillary services offered by the grid connected VSCs.

3.5.2   Protection, restoration and availability

Large-scale deployment of DC interlinks in MV-DN will require a redesign of existing AC protection systems [42]. The paper explores different fault protection strategies in such hybrid AC–DC systems using AC Circuit breakers (ACCBs), DC

Circuit Breakers (DCCBs) and fault blocking converters. The fast fault propagation in the network associated with the low impedance of DC systems, exacerbated by the slow response of ACCBs (several hundred microseconds), makes selective isolation a challenge. Nevertheless, if the embedded DC interlinks are restricted to point-to-point topology within the AC MV-DN, ACCB based solution is possible. While DCCBs and full-bridged converter based topologies can offer rapid fault-clearance time, these methods involve higher capital costs and power losses that are challenging to justify at MV-level. A promising solution based on multi-line hybrid circuit breaker minimizes the installation costs by sharing the solid-state based current commutation path for protection of several DC lines [43].

At the system level, the two important network protection requirements include (i) proper selectivity and speed to minimize the downstream load shedding and (ii) service restoration with adequate capacity during $(n-1)$ contingencies [21,44]. The former necessitates design of protection devices considering relay coordination associated with fault response time, current magnitude and direction. The latter involves the trade-offs in redundancy and reconfigurability in maintaining the required power capacity when the operation of a healthy grid section is restored post-fault isolation. The field tests conducted in [45] indicate that the maximum service restoration time including fault isolation, switch motion and system reconfiguration is 500–800 ms. It is discussed in [35] that the costs associated with the inevitable loss in load corresponding to this restoration time is negligible compared to the benefit in downsizing the redundancy requirements achieved with AC–DC reconfigurability described in Section 3.4.

Different $(n-1)$ contingencies on AC lines, DC lines, generators and converters were studied to demonstrate that the number of network violations were reduced by more than 70% when embedded DC networks were used to support the AC network for increasing the security of supply and resilience during outages [46]. Figure 3.12 (a) shows the pre-fault DN with two radial laterals with several nodal power load taps protected with protection relays R11–R14 and R21–R24. Conventionally, these
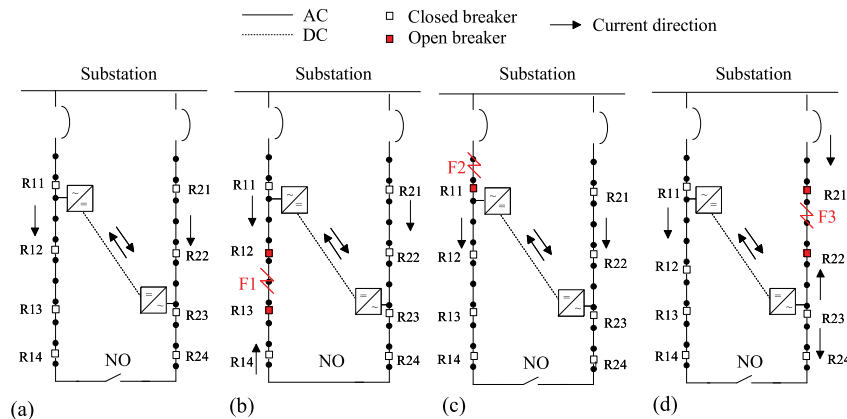

Figure 3.12   *Improving availability of the radial AC DN using DC interlinks [14]*

laterals are interconnected at end points using a NO tie-line. The tie-line is used to re-energize loads to healthy downstream section through another feeder after fault isolation. Therefore, outage management in this case needs intervention after fault clearance and the new network topology resulting with the closure of the tie switch can have high system losses, overloaded branches and poor voltage profile along the healthy feeder. A different strategy to improve availability is to weakly mesh the system by using a DC interlink with controlled bi-directional power capability, shown to be installed between relay location R11–R12 and R22–R23.

Figure 3.12(b) shows that when fault F1 is isolated using R12 and R13, the tie-switch re-energizes loads downline of R13. In this case, power redirection using the dc-interlink can prevent overloads in branches upstream of R23. Further, depending on the distance of R13 from the tie-line, the nodal voltage profile can be improved. For fault locations F2 and F3 in Figure 3.12(c) and (d), the tie-switch operation can be avoided while ensuring power availability to healthy sections. It can further be observed that the original current direction can be preserved in the active relays.

The main conclusion from this illustrative discussion is that the DC interlink can improve the system availability while minimizing the post-clearance tie-line switching operations, prevent branch overloads by introducing parallel pathways for controlled power flow and eliminate node voltage violations. However, these are competing objectives governing the optimal location and capacity of the installed dc-interlink. For example, if the NO tie-line itself is refurbished to operate as dc, switching operation can be avoided during fault F1 as well. On the other hand, the ability of the DC link to prevent branch overloads will be limited. Furthermore, it can be inferred from Section 3.3 that the system efficiency during normal operation can reduce with end-node DC link power redirection. Therefore, protection coordination and service restoration goal can add an interesting research dimension to the placement and sizing of DC power routers in radial AC distribution networks.

References

[1]   Sijm J, Gockel P, de Joode J, r van Westering W, and Musterd M. The demand for flexibility of the power system in the Netherlands, 2015−2050. In: *Report of Phase 1 of the FLEXNET Project*; 2017. pp. 1–140.

[2]   Luong NH, Grond MOW, La Poutré H, and Bosman PAN. Scalable and practical multi-objective distribution network expansion planning. In: *2015 IEEE Power Energy Society General Meeting*; 2015. pp. 1–5.

[3]   Ismael SM, Abdel Aleem SHE, Abdelaziz AY, and Zobaa AF. Practical considerations for optimal conductor reinforcement and hosting capacity enhancement in radial distribution systems. *IEEE Access*. 2018; 6: 27268–27277.

[4]   Liu Y, Cao X, and Fu M. The upgrading renovation of an existing XLPE cable circuit by conversion of AC line to DC operation. *IEEE Transactions on Power Delivery*. 2017; 32(3): 1321–1328.

[5]   Shekhar A, Kontos E, Ramírez-Elizondo L, Rodrigo-Mor A, Bauer P. Grid capacity and efficiency enhancement by operating medium voltage AC

cables as DC links with modular multilevel converters. *International Journal of Electrical Power & Energy Systems*. 2017; 93: 479–493.

[6]   Deboever J, Peppanen J, Maitra N, Damato G, Taylor J, and Pate J. Energy storage as a non - wires alternative for deferring distribution capacity investments. In: *2018 IEEE/PES Transmission and Distribution Conference and Exposition (T D)*; 2018. pp. 1–5.

[7]   Mateo C, Rodríguez Calvo A, Reneses Guillén J, Frías Marín P, and Sánchez Miralles A. Cost−benefit analysis of battery storage in medium−voltage distribution networks. *IET Generation, Transmission Distribution*. 2016; 10(3): 815–821.

[8]   Ziari I, Ledwich G, Ghosh A, and Platt G. Integrated distribution systems planning to improve reliability under load growth. *IEEE Transactions on Power Delivery*. 2012; 27(2): 757–765.

[9]   Assis TML, *et al.* Impact of multi - terminal HVDC grids on enhancing dynamic power transfer capability. *IEEE Transactions on Power Systems*. 2017; 32(4): 2652–2662.

[10] Piccolo A and Siano P. Evaluating the impact of network investment deferral on distributed generation expansion. *IEEE Transactions on Power Systems*. 2009; 24(3): 1559–1567.

[11] Zhao J, Wang J., Xu Z, Wang C, Wan C, and Chen C. Distribution network electric vehicle hosting capacity maximization: a chargeable region optimization model. *IEEE Transactions on Power Systems*. 2017; 32(5): 4119–4130.

[12] Palensky P and Dietrich D. Demand side management: demand response, intelligent energy systems, and smart loads. *IEEE Transactions on Industrial Informatics*. 2011; 7(3): 381–388.

[13] Dragičević T, Wheeler P, and Blaabjerg F. *DC Distribution Systems and Microgrids*. The Institution of Engineering and Technology (IET). 2018. pp. 1–469.

[14] Shekhar A, Ramírez-Elizondo L, Feng X, Kontos E, and Pavol B. Reconfigurable DC links for restructuring existing medium voltage AC distribution grids. *Electric Power Components and Systems*. 2017; 45(16): 1739–1746.

[15] Rentschler A, Kuhn G, Delzenne M, and Kuhn O. Medium voltage DC, challenges related to the building of long overhead lines. In: *2018 IEEE/PES Transmission and Distribution Conference and Exposition (T D)*; 2018. pp. 1–5.

[16] Shekhar A, Kontos E, Mor AR, Ramírez-Elizondo L, and Bauer P. Refurbishing existing MVAC distribution cables to operate under DC conditions. In: *2016 IEEE International Power Electronics and Motion Control Conference (PEMC)*; 2016. pp. 450–455.

[17] Zhang L, Liang J, Tang W, Li G, Cai Y, and Sheng W. Converting AC distribution lines to DC to increase transfer capacities and DG penetration. *IEEE Transactions on Smart Grid*. 2019; 10(2): 1477–1487.

[18] Larruskain DM, Zamora I, Abarrategui O, and Aginako Z. Conversion of AC distribution lines into DC lines to upgrade transmission capacity. *Electric Power Systems Research*. 2011; 81(7): 1341–1348.

[19] Clerici A, Paris L, and Danfors P. HVDC conversion of HVAC lines to provide substantial power upgrading. *IEEE Transactions on Power Delivery*. 1991; 6(1): 324–333.

[20]   Shekhar A, Feng X, Gattozzi A, *et al.* Impact of DC voltage enhancement on partial discharges in medium voltage cable–an empirical study with defects at semicon-dielectric Interface. *Energies*. 2017; 10(12): 1968.

[21]   Shekhar A, Kontos E, Ramírez-Elizondo LM, and Bauer P. Ac distribution grid reconfiguration using flexible DC link architecture for increasing power delivery capacity during $(n-1)$ contingency. In: *2017 IEEE Southern Power Electronics Conference (SPEC)*.IEEE; 2017. pp. 1–6.

[22]   Shekhar A, Ramírez-Elizondo LM, Batista T, and Bauer P. Boundaries of operation for refurbished parallel AC-DC reconfigurable links in distribution grids. *IEEE Transactions on Power Delivery*. 2020; 35(2): 549–559.

[23]   Shekhar A, Ramirez-Elizondo L. and Bauer P. Reliability, efficiency and cost trade-offs for medium voltage distribution network expansion using refurbished AC–DC reconfigurable links. In: *2018 International Symposium on Power Electronics, Electrical Drives, Automation and Motion (SPEEDAM)*. IEEE; 2018. pp. 242–247.

[24]   Larruskain DM, Zamora I, Abarrategui O, and Iturregi A. VSC-HVDC configurations for converting AC distribution lines into DC lines. *International Journal of Electrical Power & Energy Systems*. 2014; 54: 589–597.

[25]   Yazdani A and Iravani R. *Voltage-Sourced Converters in Power Systems*. John Wiley & Sons Inc; 2010. pp. 127–159.

[26]   Ma K and Blaabjerg F. Multilevel converters for 10 MW wind turbines. In: *Proceedings of the 2011 14th European Conference on Power Electronics and Applications*; 2011. pp. 1–10.

[27]   Huber JE and Kolar JW. Optimum number of cascaded cells for high-power medium-voltage AC–DC converters. *IEEE Journal of Emerging and Selected Topics in Power Electronics*. 2017; 5(1): 213–232.

[28]   Shekhar A, Soeiro TB, Qin Z, Ramirez Elizondo LM, and Bauer P. Suitable submodule switch rating for medium voltage modular multilevel converter design. In: *2018 IEEE Energy Conversion Congress and Exposition (ECCE)*; 2018. pp. 3980–3987.

[29]   Shekhar A, Larumbe LB, Soeiro TB, Wu Y, and Bauer P. Number of levels, arm inductance and modulation trade-offs for high power medium voltage grid-connected modular multilevel converters. In: *2019 10th International Conference on Power Electronics and ECCE Asia (ICPE 2019 – ECCE Asia)*; 2019. pp. 1–8.

[30]   Morshuis PHF and Smit JJ. Partial discharges at DC voltage: their mechanism, detection and analysis. *IEEE Transactions on Dielectrics and Electrical Insulation*. 2005; 12(2): 328–340.

[31]   Stancu C and Notingher P. Computation of the electric field in aged underground medium voltage cable insulation. *IEEE Transactions on Dielectrics and Electrical Insulation*. 2013; 20(5): 1530–1539.

[32]   Uehara H, Li Z, Cao Y, Chen Q, and Montanari GC. The effect of thermal gradient on space charge pattern in XLPE. In: *2015 IEEE Conference on Electrical Insulation and Dielectric Phenomena (CEIDP)*; 2015. pp. 138–141.

[33] Tefferi M, Li Z, Uehara H, Chen Q, and Cao Y. Characterization of space charge and DC field distribution in XLPE and EPR during voltage polarity reversal with thermal gradient. In: *2017 IEEE Conference on Electrical Insulation and Dielectric Phenomenon (CEIDP)*; 2017. pp. 617–620.

[34] Shekhar A, Soeiro TB, Wu Y, and Bauer P. Optimal power flow control in parallel operating AC and DC distribution links. *IEEE Transactions on Industrial Electronics*. 2021; 68(2): 1695–1706.

[35] Shekhar A, Soeiro TB, Ramírez-Elizondo LM, and Bauer P. Offline reconfigurability based substation converter sizing for hybrid AC−DC distribution links. *IEEE Transactions on Power Delivery*. 2020; 33(5): 2342–2352.

[36] Shekhar A, Soeiro TB, Ramírez-Elizondo L, and Bauer P. *Weakly Meshing the Radial Distribution Networks with Power Electronic Based Flexible DC Interlinks*. ICDCM. 2019.

[37] Baran ME and Wu FF. Network reconfiguration in distribution systems for loss reduction and load balancing. *IEEE Transactions on Power Delivery*. 1989; 4(2): 1401–1407.

[38] Jiang D and Baldick R. Optimal electric distribution system switch reconfiguration and capacitor control. *IEEE Transactions on Power Systems*. 1996; 11(2): 890–897.

[39] Shirmohammadi D and Hong HW. Reconfiguration of electric distribution networks for resistive line losses reduction. *IEEE Transactions on Power Delivery*. 1989; 4(2): 1492–1498.

[40] Romero-Ramos E, Gomez-Exposito A, Marano-Marcolini A and Maza-Ortega JM. Assessing the loadability of active distribution networks in the presence of DC controllable links. *IET Generation, Transmission Distribution*. 2011; 5(11): 1105–1113.

[41] Chaudhary SK, Guerrero J, and Teodorescu R. Enhancing the capacity of the AC distribution system using DC interlinks−a step toward future DC grid. *IEEE Transactions on Smart Grid*. 2015; 6(4): 1722–1729.

[42] Li G, Zhang L, Joseph T, Liang J and Yan G. Comparisons of MVAC and MVDC systems in dynamic operation, fault protection and post-fault restoration. In: *IECON 2019 - 45th Annual Conference of the IEEE Industrial Electronics Society*. Vol. 1; 2019. p. 5657–5662.

[43] Kontos E, Schultz T, Mackay L, Ramirez-Elizondo L, Franck C, and Bauer P. Multiline breaker for HVDC applications. *IEEE Transactions on Power Delivery*. 2018; 33(3): 1469–1478.

[44] Burstein AW, Cuk V, and de Jong ECW. Effect of network protection requirements on the design of a flexible AC/DC-link. *The Journal of Engineering*. 2018; 2018(15): 1291–1296.

[45] Yip T, Jing-huan Wang, Bingyin Xu, Kaijun Fan, and Tianyou Li. Fast self-healing control of faults in MV networks using distributed intelligence. *CIRED − Open Access Proceedings Journal*. 2017; 2017(1): 1131–1133.

[46] Teixeira Pinto R, Aragüés Peñalba M, Gomis Bellmunt O and Sumper A. Optimal operation of DC networks to support power system outage management. *IEEE Transactions on Smart Grid*. 2016; 7(6): 2953–2961.